Hindawi Publishing Corporation
Mathematical Problems in Engineering
Volume 2014, Article ID 418040, 9 pages
http://dx.doi.org/10.1155/2014/418040

Research Article

Fuzzy Neural Network-Based Damage Assessment of Bridge under Temperature Effect

Yubo Jiao, Hanbing Liu, Yongchun Cheng, Xianqiang Wang, Yafeng Gong, and Gang Song

College of Transportation, Jilin University, No. 5988 Renmin Street, Changchun 130025, China

Correspondence should be addressed to Yubo Jiao; jiaoyubo86@163.com

Received 24 July 2013; Revised 16 December 2013; Accepted 30 December 2013; Published 5 March 2014

Academic Editor: Yuri Petryna

Vibration-based method has been widely applied for damage identification of bridge. Natural frequency, mode shape, and their derivatives are sensitive parameters to damage. However, these parameters can be affected not only by the health of structure, but also by the changing temperature. It is essential to eliminate the influence of temperature in practice. Therefore, a fuzzy neural network-based damage assessment method is proposed in this paper. Uniform load surface curvature is used as damage indicator. Elasticity modulus of concrete is assumed to be temperature dependent in the numerical simulation of bridge model. Through selecting temperature and uniform load surface curvature as input variables of fuzzy neural network, the algorithm can distinguish the damage from temperature effect. Comparative analysis between fuzzy neural network and BP network illustrates the superiority of the proposed method.

1. Introduction

Bridge structure is playing significant role in modern transport system and economic development. With the rapid growth of traffic volume, the loads carried by bridges increase dramatically. External environment also exacerbates the deterioration of materials. Damage inevitably occurs in structures under the coupling effect of load and environment, which will lead to the deficiency of carrying capacity [1, 2]. Therefore, it is necessary to identify the structural damage and strengthen the bridge. The research on appropriate damage identification methods has received extensive attention [3, 4].

Vibration tests have been widely performed in bridge health monitoring. The dynamic characteristics such as eigenfrequencies, modal shapes, and damping ratios of structure contain effective information on bridge health status [5]. Vibration-based damage identification methods are proved feasible in laboratory and field testing. The theoretical background is that damage will modify the stiffness and mass of structure and then alter the modal data. Conversely, modal parameters can be regarded as damage indicators of structure [6]. However, these indicators are sensitive to not only damage, but also environmental conditions such as humidity, wind, and, most important, temperature [7, 8]. Wahab and de Roeck [9] conducted dynamic tests for a prestressed concrete bridge in spring and in winter and observed a change of 4%~5% in natural frequencies. Farrar et al. [10] found that the first eigenfrequency of Alamosa Canyon Bridge varies by approximately 5% during a 24 h time period. Zhou et al. [11] obtained 770 h modal frequencies and temperature data from the instrumented cable-stayed Ting Kau Bridge in Hongkong; the environmental variation accounts for changes in modal frequencies of 0.005 Hz and 0.018 Hz in absolute sense and 1.505% to 6.689% in relative sense for the first eight modes. Moser and Moaveni [12] presented results from a continuous monitoring system installed on Dowling Hall Footbridge. Significant variability in the identified natural frequencies is observed; these changes in natural frequencies are strongly correlated with temperature. Therefore, temperature effect must be effectively considered in practical application of damage identification.

Some researches have been conducted to solve this problem in recent years. One of the methods is to search the correlation between eigenfrequencies and corresponding

temperatures [13–15]. Peeters and Roeck [13] adopted a Black-box model to describe the variations of eigenfrequencies as a function of temperature. Damage can be detected if eigenfrequencies of the new data exceed certain confidence intervals of the model. Sohn et al. [14] presented a linear adaptive model to discriminate the changes of natural frequencies due to temperature changes from those caused by structural damage or other environmental effects. Peeters et al. [15] used the ARX models to simulate the eigenfrequencies. If a new measured eigenfrequency lies outside the estimated confidence intervals, it is likely that the bridge is damaged. Z24 Bridge verified its feasibility. However, this kind of method possesses several drawbacks [16, 17]. Firstly, the optimal locations of temperature sensors may be difficult to determine. Secondly, the definition of environmental variables which affect the structural features is difficult. Moreover, it would be difficult for sensors to monitor environmental variables over a long time. Another group of methods can minimize the environmental effect without measuring temperatures. Yan et al. [16] proposed a principal-component-analysis- (PCA-) based method to distinguish between changes of modal data due to environmental variation and structural damage under linear or weakly nonlinear cases. In a companion paper [18], they conducted a further extension of the proposed method to handle nonlinear cases, which may be encountered in some complex structures. Sohn et al. [7] developed a novel detection technique which can take into account the environmental conditions of system in order to minimize false positive indications. Autoassociative neural networks are employed to discriminate system changes of interest such as structural damage from other variations. As pointed out by Meruane and Heylen [19], these methods cannot identify the damage location and severity. They proposed a damage detection method which is able to deal with temperature variations. The objective function correlates mode shapes and natural frequencies, and a parallel genetic algorithm handles the inverse problem.

In this paper, a fuzzy neural network-based damage assessment method which can eliminate the temperature effect is proposed. Adaptive network-based fuzzy inference system (ANFIS) is a fuzzy inference system implemented in the framework of adaptive networks, which avoids the complexity and difficulty of traditional neural networks. Meanwhile, it can also overcome the shortcoming of poor learning ability for traditional fuzzy inference system [20]. Uniform load surface (ULS) is a derivative from modal flexibility, which is found to have much less truncation effect and is least sensitive to experimental error [21]. Therefore, ULS parameter is selected as damage indicator. Pham [22] pointed out that the changes of ambient temperature mainly affect the elastic modulus of the construction material and therefore the stiffness of the entire bridge. Shoukry et al. [23] obtained the relationship between temperature and elastic modulus of concrete. The numerical model of structure assumes that the elastic modulus of the materials is temperature dependent. Through considering temperature and ULS parameter in the calculating process of ANFIS, it can distinguish the damage from temperature effect. In order to verify its superiority, comparative analysis between fuzzy neural network and BP network is conducted.

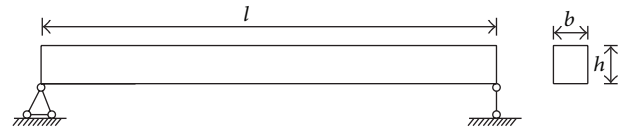

Figure 1: Diagram of simply supported Euler-Bernoulli beam.

2. Theoretical Background

2.1. Dynamics Background under Temperature Effect. According to existing research results, temperature alters the modal parameters through a complicated way. On one hand, temperature effect will affect mechanical properties of materials. On the other hand, the geometry is sensitive to temperature, which will change constraint conditions. A simply supported Euler-Bernoulli beam with uniform section shown in Figure 1 is considered for modal analysis under temperature effect.

It is assumed that mass and constraint conditions remain unchanged and temperature only affects the geometry and mechanical properties. The undamped flexural vibration frequency of order n for beam structure can be calculated by [24–27]

$$f_n = \frac{n^2\pi h}{2l^2}\sqrt{\frac{E}{12\rho}}, \tag{1}$$

where l and h are the length and height of beam, respectively. ρ is material density and E is elastic modulus.

According to variational principles [28], it can be obtained that

$$\begin{aligned}\delta f_n = {} & (\delta h)\frac{n^2\pi}{2l^2}\sqrt{\frac{E}{12\rho}} + \left(-2l^{-3}\cdot\delta l\right)\frac{n^2\pi h}{2}\sqrt{\frac{E}{12\rho}} \\ & + \left(\frac{1}{2}E^{-1/2}\cdot\delta E\right)\frac{n^2\pi h}{2l^2}\sqrt{\frac{1}{12\rho}} \\ & + \left(-\frac{1}{2}\rho^{-3/2}\cdot\delta\rho\right)\frac{n^2\pi h}{2l^2}\sqrt{\frac{E}{12}},\end{aligned} \tag{2}$$

where δ represents an increment in the corresponding parameters.

Therefore, it can be furtherly derived that

$$\begin{aligned}\frac{\delta f_n}{f_n} &= \frac{\delta f_n}{\left(\left(n^2\pi h/2l^2\right)\sqrt{E/12\rho}\right)} \\ &= \frac{\delta h}{h} - 2\frac{\delta l}{l} + \frac{1}{2}\frac{\delta E}{E} - \frac{1}{2}\frac{\delta\rho}{\rho}.\end{aligned} \tag{3}$$

Table 1: Temperature-elastic modulus data obtained by Shoukry et al. [23].

Temperature (°C)	−20	−10	0	10	20
Elastic modulus ($\times 10^{10}$ Pa)	2.937	2.855	2.744	2.703	2.523

Assuming that the thermal coefficient of linear expansion of the material is θ_t and the temperature coefficient of modulus is θ_E, it can be obtained that

$$\frac{\delta h}{h} = \theta_t \delta t, \qquad \frac{\delta l}{l} = \theta_t \delta t,$$
$$\frac{\delta \rho}{\rho} = -3\theta_t \delta t, \qquad \frac{\delta E}{E} = \theta_E \delta t. \tag{4}$$

Here we assume that the variation of modulus with temperature is linear for small changes in temperature. Consider the following:

$$\frac{\delta f_n}{f_n} = \frac{1}{2}\left(\theta_t + \theta_E\right)\delta t. \tag{5}$$

It can be seen from (5) that $\theta_t \approx 1.0 \times 10^{-5}/^{\circ}\mathrm{C}$ and $\theta_E \approx -4.5 \times 10^{-3}/^{\circ}\mathrm{C}$ for concrete under 100°C, $\theta_E \gg \theta_t$ [25]. Therefore, modulus of concrete is the main factor altering the modal frequency.

In above calculation, constraint condition is not considered. The axial force exerted on both ends of the beam is

$$F = \frac{1}{2}\mu mg, \tag{6}$$

where μ is the friction coefficient and mg is weight of the beam.

According to modal analysis, natural frequency of beam under axial force can be calculated by

$$f_n' = f_n\sqrt{1 + \frac{Fl^2}{n^2\pi^2 EI}}, \tag{7}$$

where I is moment of inertia. Assuming that $\mu = 0.5$, (7) can be transformed into

$$f_n' = \omega_n\sqrt{1 + \frac{mgl^2}{4n^2\pi^2 EI}} = f_n\sqrt{1 + \frac{1}{n^2}\cdot\frac{mgl^2}{4\pi^2 EI}}, \tag{8}$$

where $mgl^2 \ll 4\pi^2 EI$, $\sqrt{1 + (1/n^2)\cdot(mgl^2/4\pi^2 EI)} \approx 1$, so constraint condition has little influence on modal frequency.

Through above theoretical analysis, we can obtain that temperature effect alters modal frequency mainly by changing the elastic modulus of concrete. Shoukry et al. [23] got the relationship between temperature and modulus by laboratory tests which are listed in Table 1. Based on the research results, an ANFIS-based temperature effect elimination method is proposed.

2.2. Adaptive Network-Based Fuzzy Inference System (ANFIS). Taking the fuzzy inference system with two inputs (x, y) and one output, for example, the if-then rules are listed as follows [20].

Rule 1: if x is A_1 and y is B_1, then $f_1 = p_1\cdot x + q_1\cdot y + r_1$.

Rule 2: if x is A_2 and y is B_2, then $f_2 = p_2\cdot x + q_2\cdot y + r_2$,

where x, y are input variables for nodes, symbols A_1, A_2, B_1, and B_2 are linguistic expressions, f_1 and f_2 are output variables and p_1, q_1, r_1, p_2, q_2, r_2 are parameters.

The fuzzy inference mechanism of Sugeno model is shown in Figure 2, and the equivalent structure for ANFIS is shown in Figure 3. The same membership functions are adopted, and the output for ith node at lth layer is represented by $O_{l,i}$.

Layer 1: every node i in this layer has a corresponding node function.

$$O_{1,i} = \mu_{A_i}(x), \quad i = 1, 2,$$
$$O_{1,i} = \mu_{B_{i-2}}(y), \quad i = 3, 4, \tag{9}$$

where symbols A, B are linguistic expressions (such as "small" or "large"). $O_{1,i}$ is membership degree for fuzzy set $A = (A_1, A_2, B_1, B_2)$; it specifies the degree to which the given inputs x and y satisfy the quantifier A. $\mu(x)$ is membership function which can be Bell, Sigmoid, or other related functions.

Layer 2: nodes in this layer are all fixed nodes represented by Π, and the output is the product of all inputs. Consider the following:

$$O_{2,i} = \omega_{A_i}(x)\,\mu_{B_i}(y), \quad i = 1, 2. \tag{10}$$

Output of each node represents the incentive intensity for one rule. Generally, the node function can be T-Norms operators.

Layer 3: nodes in this layer are all fixed nodes represented by N. The ith node is used for getting the normalized incentive intensity. Consider the following:

$$O_{3,i} = \bar{\omega} = \frac{\omega_i}{\omega_1 + \omega_2}, \quad i = 1, 2. \tag{11}$$

Layer 4: nodes in this layer are adaptive nodes with corresponding function. Consider the following:

$$O_{4,i} = \overline{\omega} \times f_i = \overline{\omega} \times \left(p_i x + q_i y + r_i\right), \quad i = 1, 2, \tag{12}$$

where $\overline{\omega}$ are normalized incentive intensity calculated by (11) and $\{p_i, q_i, r_i\}$ are parameters.

Layer 5: this layer is with only one node and labeled by $\sum$, which is used to calculate the transferred message and acts as the overall output.

$$\text{Overall output} = O_{5,i} = \sum \overline{\omega_i} \times f_i = \frac{\sum_i \overline{\omega_i} \times f_i}{\sum_i \overline{\omega_i}}. \tag{13}$$

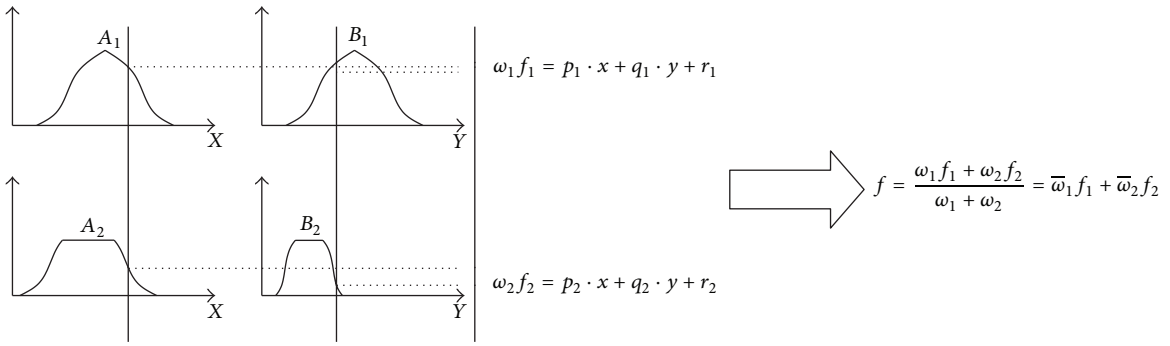

Figure 2: One-order Sugeno model with two rules and inputs.

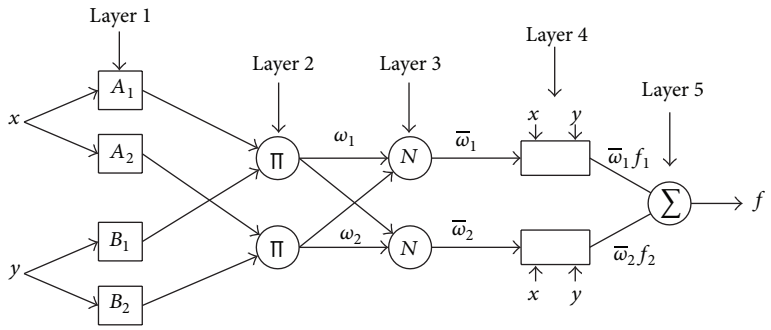

Figure 3: Basic structure of ANFIS.

2.3. Uniform Load Surface (ULS). The modal flexibility matrix can be calculated by (14) based on natural frequencies and mode shapes [21]. Consider the following:

$$f_{i,j} = \sum_{k=1}^{m} \frac{\phi^k(i)\,\phi^k(j)}{\omega_k^2}, \tag{14}$$

where ϕ is mass normalized mode shape vector, ω is natural frequency, k is the order of modal data, i and j are node numbers, m is the totally orders needed for calculation of modal flexibility matrix. It can be seen from (14) that the modal contribution to flexibility matrix decreases rapidly as the frequencies increase, so the flexibility matrix converges rapidly as the number of contributing lower modes increases. It reveals that an approximation of flexibility matrix can be obtained through several lower modes.

The deflection vector $\{\overline{f}\}$ under uniform load which is called the uniform load surface [27] can be calculated by

$$\left\{\overline{f}\right\} = \begin{bmatrix} f_{11} & f_{12} & \cdots & f_{1n} \\ f_{21} & f_{22} & \cdots & f_{2n} \\ \vdots & \vdots & \vdots & \vdots \\ f_{n1} & f_{n2} & \cdots & f_{nn} \end{bmatrix} \begin{Bmatrix} 1 \\ 1 \\ \vdots \\ 1 \end{Bmatrix}, \tag{15}$$

where

$$\begin{aligned} \overline{f}(i) &= \sum_{j=1}^{n} f_{i,j} = \sum_{j=1}^{n} \left(\sum_{k=1}^{m} \frac{\phi^k(i)\,\phi^k(j)}{\omega_k^2} \right) \\ &= \sum_{k=1}^{m} \frac{\phi^k(i) \sum_{j=1}^{n} \phi^k(j)}{\omega_k^2}. \end{aligned} \tag{16}$$

Uniform load surface curvature (ULSC) can be obtained by the second order differential of $\{\overline{f}\}$, as shown in the following equation:

$$\text{ULSC} = \frac{\overline{f}(i+1) + \overline{f}(i-1) - 2 \times \overline{f}(i)}{l^2}, \tag{17}$$

where l is the element length.

The uniform load surface curvature difference (ULSCD) can be calculated by

$$\text{ULSCD} = \text{ULSC}^d - \text{ULSC}^u, \tag{18}$$

where ULSC^u, ULSC^d are the uniform load surface curvatures before and after damage, respectively.

Numerical simulation is conducted for a simply supported beam with rectangular cross-section in order to verify the effectiveness of ULS parameters. The length (L) is 9.0 m; the width (B) and height (H) of cross-section are 0.6 m and 1.0 m, respectively. The material is concrete with the compressive strength of 30 Mpa and density of 2500 kg/m^3. Finite element model is constructed by ANSYS; it includes 15 elements and 16 nodes with element length of 0.6 m (Figure 4).

The damage severity of structure is represented by reduction in the element stiffness and it can be defined by

$$D = \frac{\left(E^u - E^d\right)}{E^u}, \tag{19}$$

where D represents the damage severity of elements, E is Young's modulus of the bridge material, and the superscripts

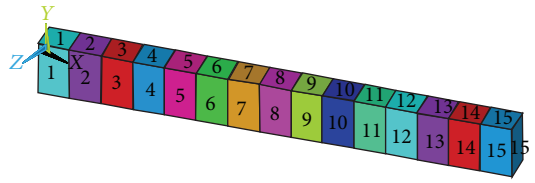

Figure 4: Finite element simulation for simply supported bridge with uniform section.

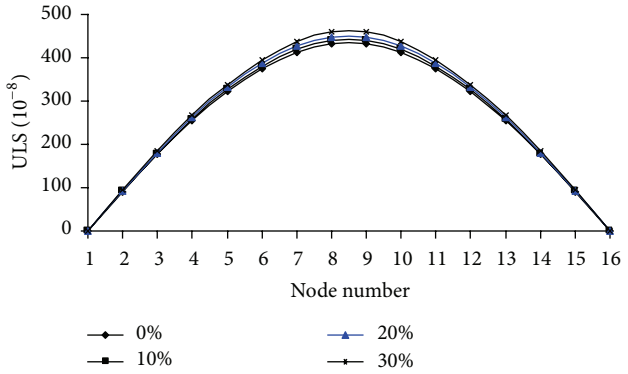

Figure 5: Relationship between ULS index and damage severity.

u and d represent undamaged and damaged elements, respectively.

Taking the damage identification of element 8 with damage severity of 0%, 10%, 20%, and 30% at temperature 30°C, for example, the ULS, ULSC, and ULSCD parameters can be calculated by (15)~(18); they are shown in Figures 5, 6, and 7.

As can be seen from Figures 5~7, ULS parameter can be used to identify the damage occurrence, while ULSC and ULSCD can localize the damage, and ULSCD possesses better effect.

3. Numerical Simulation for Damage Identification Based on ANFIS

3.1. Damage Identification Process and Characteristic Parameters. The specific calculation process for ANFIS-based damage identification is shown in Figure 8.

The normalized temperature and ULSCD parameters are selected as input variables of ANFIS, while damage severity of element is output one. Consider the following:

$$\text{Input} = \left\{\overline{T}, \overline{\text{ULSCD}_1}, \overline{\text{ULSCD}_2}, \ldots, \overline{\text{ULSCD}_n}\right\}, \quad (20)$$

where $\overline{\text{ULSC}_i}$ is normalized ULSCD vector and $\overline{T}$ is normalized temperature vector.

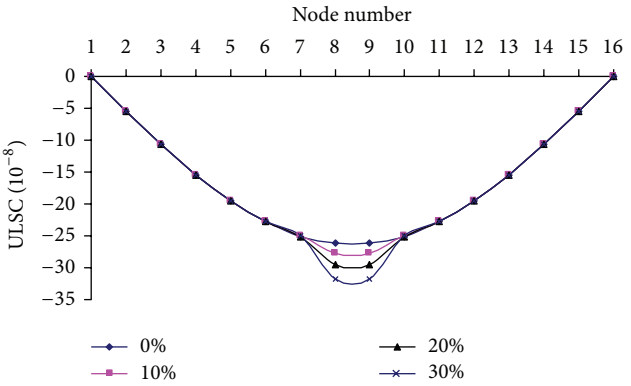

Figure 6: Relationship between ULSC and damage severity.

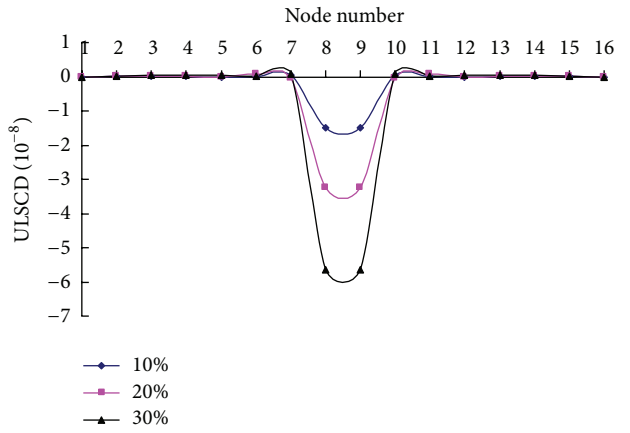

Figure 7: Relationship between ULSCD and damage severity.

Taking the damage identification of element 8, for example, its input variable can be represented by

$$\text{Input} = \left\{\overline{T}, \overline{\text{ULSCD}_8}\right\}. \quad (21)$$

Membership function for input variable is Gauss type; ANFIS can be initialized by fuzzy-C clustering. The ANFIS structure used in this paper is shown in Figure 9.

3.2. ANFIS-Based Damage Assessment under Temperature Effect. In order to determine the parameters of ANFIS, certain numbers of training samples are needed to realize the adjustment and optimization. 15 samples listed in Table 2 are selected for training and forming the ANFIS structure.

A hybrid learning algorithm based on back propagation and least squares is used for training, which can adjust the premise and conclusion parameters and produce if-then rule base automatically.

ANFIS can achieve adaptive adjustment of membership functions. The same initial function is adopted for input and output variables; it is shown in Figure 10.

The membership functions for input variables ($\overline{T}$ and $\overline{\text{ULSCD}_8}$) after training are shown in Figures 11 and 12.

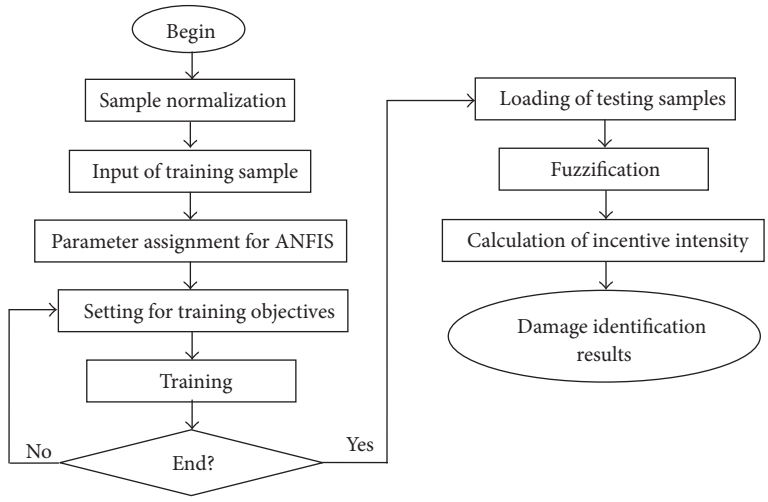

Figure 8: Damage identification process of ANFIS.

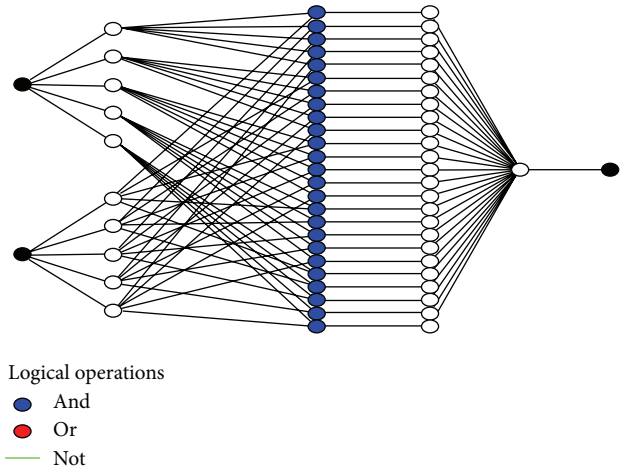

Figure 9: Structure for damage identification of ANFIS.

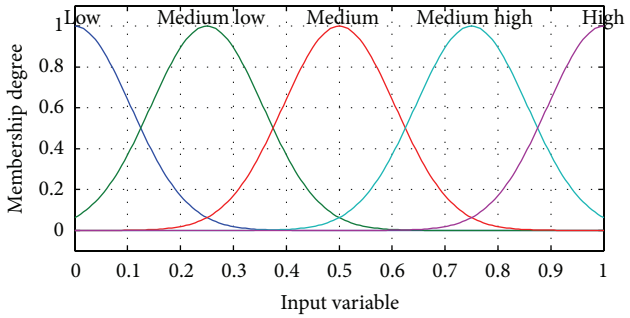

Figure 10: Membership function of input variables before training.

Test samples are constructed to verify the feasibility of ANFIS. The test samples and corresponding identification results are listed in Table 3.

As can be seen from Table 3, the proposed method in this paper can effectively identify the damage condition of bridge.

Table 2: Cases for training.

Temperature (°C)	Damage severity	$ULSCD_8$ (10^{-8})	Damage condition
−20	10%	−1.3097	Slight damage
	20%	−2.8716	Moderate damage
	30%	−4.9760	Severe damage
−10	10%	−1.3488	Slight damage
	20%	−2.9618	Moderate damage
	30%	−5.1336	Severe damage
0	10%	−1.4048	Slight damage
	20%	−3.0803	Moderate damage
	30%	−5.3394	Severe damage
10	10%	−1.4256	Slight damage
	20%	−3.1265	Moderate damage
	30%	−5.4208	Severe damage
20	10%	−1.5260	Slight damage
	20%	−3.3502	Moderate damage
	30%	−5.8044	Severe damage

It reveals that ANFIS can realize the adaptive identification and possesses favorable accuracy.

4. Comparative Analysis between ANFIS and BP Networks

4.1. Damage Identification Based on BP Networks under Temperature Effect. Changes of frequencies are used as damage identification parameters; it can be calculated by

$$\Delta\omega_i = \omega^u - \omega^d, \tag{22}$$

where ω^u and ω^d are natural frequencies before and after damage, respectively.

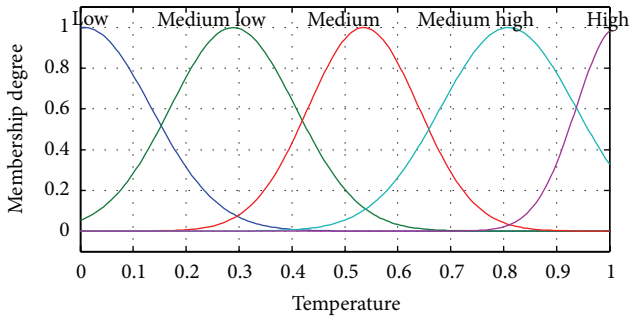

Figure 11: Membership function of $\overline{T}$ after training.

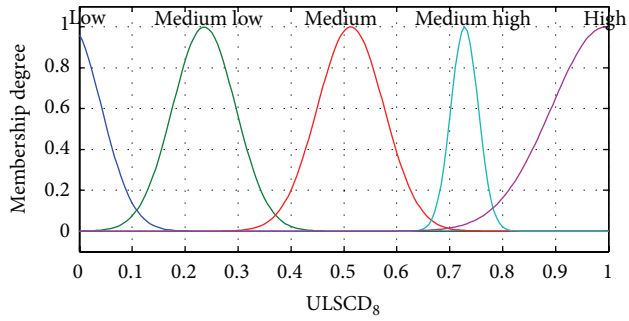

Figure 12: Membership function of $\overline{\text{ULSCD}_8}$ after training.

The input variable for BP neural networks is shown in the following equation:

$$\text{Input} = \{T, \Delta\omega_1, \Delta\omega_2, \Delta\omega_3, \Delta\omega_4\}. \quad (23)$$

Under the temperatures −20°C, −10°C, 0°C, 10°C, and 20°C, damage severity of 5%, 10%, 15%, and 20% for each element of 4, 6, and 8 is selected as training samples, while 7%, 12%, and 18% are test samples. The identification results are listed in Table 4.

The maximum relative error for BP neural networks-based damage assessment is 5.17%; the identification results are satisfactory.

4.2. Comparison of Identification Accuracy between ANFIS and BP. Comparative analysis is conducted in order to compare the superiority between BP-frequency and ANFIS-ULS-based methods. A similarity calculation formula is constructed to conduct evaluation considering the dimension difference between two methods. Consider the following:

$$d\left(R^E, R^A\right) = \sqrt{\frac{\sum_{i=1}^{n}\left[\left(R_i^E - R_i^A\right)/R_i^E\right]^2}{n}}, \quad (24)$$

where R^E and R^A are the expected and actual outputs of damage identification, respectively. $d(R^E, R^A)$ represents the distance between R^E and R^A. The bigger the $d(R^E, R^A)$ is, the lower the relevance between R^E and R^A is. n is the number of test samples.

According to (24) and Tables 3 and 4, the similarities are calculated for the identification results of BP and ANFIS.

Table 3: Cases for testing and identification results of ANFIS.

Temperature (°C)	Damage severity	ULSCD_8 (10^{-8})	Expected outputs	Actual results
−20	12%	−1.61	1	1.03
−10	18%	−2.63	2	1.95
0	8%	−1.09	1	0.98
10	27%	−4.70	3	3.04
20	23%	−4.06	2	2.05
−8	10%	−1.41	1	1.05
16	19%	−3.10	2	1.97

Table 4: Damage severity identification based on frequency and neural network.

Damaged elements	Damage severity (%)	Temperature (°C)	Identification results (%)	Relative error (%)
4	7	10	7.11	1.57
		20	6.79	3.00
	12	10	12.21	1.75
		20	12.32	2.67
	18	10	18.32	1.78
		20	17.68	1.78
6	7	10	7.31	4.43
		20	7.24	3.43
	12	10	11.56	3.67
		20	11.58	3.50
	18	10	17.28	4.00
		20	18.26	1.44
8	7	10	7.18	2.57
		20	7.23	3.29
	12	10	11.69	2.58
		20	12.62	5.17
	18	10	18.55	3.06
		20	18.82	4.56

$d(R^E, R^A)_{\text{BP}} = 0.032$, $d(R^E, R^A)_{\text{ANFIS}} = 0.028$, and $d(R^E, R^A)_{\text{ANFIS}} < d(R^E, R^A)_{\text{BP}}$. Therefore, the identification results of ANFIS are more relevant to the expected results. It reveals that ANFIS possesses more favorable accuracy.

5. Conclusions

Temperature effect can cause abnormal changes of modal parameters, which will lead to incorrect damage identification results. This paper presents an effective strategy for eliminating temperature effect in damage identification of bridge. ANFIS combines the advantages of neural networks and fuzzy inference system, which is used as damage identification algorithm. ULS, ULSC, and ULSCD are proved to localize damage locations accurately; ULSCD possesses more favorable effect. Therefore, temperature and ULSCD are treated as input variables of ANFIS for the damage assessment. In numerical simulation, elastic modulus of concrete

is assumed to be temperature dependent; 15 samples are used for training and constructing ANFIS structure. Numerical simulation results reveal that the proposed method can effectively identify the damage condition of test samples. Comparative analysis is conducted for comparing the superiority between BP and ANFIS. A similarity calculation formula is constructed for evaluation, and the comparative analysis reveals that ANFIS results are more relevant to actual situation. It means that the proposed method in this paper possesses more favorable accuracy than BP network.

Considering the complexity of damage identification of bridge under temperature effect, the damage identification with more samples and damaged elements should be conducted in the future.

Conflict of Interests

The authors declare that there is no conflict of interests regarding the publication of this paper.

Acknowledgments

The authors express their appreciation for the financial support of National Natural Science Foundation of China under Grant nos. 51378236 and 51278222 and "985 Project" of Jilin University.

References

[1] K. Dems and Z. Mróz, "Damage identification using modal, static and thermographic analysis with additional control parameters," *Computers & Structures*, vol. 88, no. 21-22, pp. 1254–1264, 2010.

[2] A. D. Orcesi and D. M. Frangopol, "Optimization of bridge maintenance strategies based on structural health monitoring information," *Structural Safety*, vol. 33, no. 1, pp. 26–41, 2011.

[3] J. M. Ko and Y. Q. Ni, "Technology developments in structural health monitoring of large-scale bridges," *Engineering Structures*, vol. 27, no. 12, pp. 1715–1725, 2005.

[4] L. A. Overbey and M. D. Todd, "Effects of noise on transfer entropy estimation for damage detection," *Mechanical Systems and Signal Processing*, vol. 23, no. 7, pp. 2178–2191, 2009.

[5] K. Zhang, H. Li, Z. D. Duan, and S. S. Law, "A probabilistic damage identification approach for structures with uncertainties under unknown input," *Mechanical Systems and Signal Processing*, vol. 25, no. 4, pp. 1126–1145, 2011.

[6] H. P. Chen, "Application of regularization methods to damage detection in large scale plane frame structures using incomplete noisy modal data," *Engineering Structures*, vol. 30, no. 11, pp. 3219–3227, 2008.

[7] H. Sohn, K. Worden, and C. F. Farrar, "Novelty detection under changing environmental conditions," in *Smart Structures and Materials 2001: Smart Systems for Bridges, Structures, and Highways*, vol. 4330 of *Proceedings of SPIE*, pp. 108–118, Newport Beach, Calif, USA, March 2001.

[8] Y. Q. Ni, X. G. Hua, K. Q. Fan, and J. M. Ko, "Correlating modal properties with temperature using long-term monitoring data and support vector machine technique," *Engineering Structures*, vol. 27, no. 12, pp. 1762–1773, 2005.

[9] M. A. Wahab and G. de Roeck, "Effect of temperature on dynamic system parameters of a highway bridge," *Structural Engineering International*, vol. 7, no. 4, pp. 266–270, 1997.

[10] C. Farrar, S. Doebling, P. Cornwell, and E. Straser, "Variability of modal parameters measured on the Alamosa Canyon Bridge," in *International Society for Optical Engineering*, vol. 3089 of *Proceedings of SPIE*, pp. 257–263, Orlando, Fla, USA, February 1997.

[11] H. F. Zhou, Y. Q. Ni, and J. M. Ko, "Constructing input to neural networks for modeling temperature-caused modal variability: mean temperatures, effective temperatures, and principal components of temperatures," *Engineering Structures*, vol. 32, no. 6, pp. 1747–1759, 2010.

[12] P. Moser and B. Moaveni, "Environmental effects on the identified natural frequencies of the Dowling Hall Footbridge," *Mechanical Systems and Signal Processing*, vol. 25, no. 7, pp. 2336–2357, 2011.

[13] B. Peeters and G. D. Roeck, "One-year monitoring of the Z24-Bridge: environmental effects versus damage events," *Earthquake Engineering & Structural Dynamics*, vol. 30, no. 2, pp. 149–171, 2001.

[14] H. Sohn, M. Dzwonczyk, E. G. Straser, A. S. Kiremidjian, K. Law, and T. Meng, "An experimental study of temperature effect on modal parameters of the Alamosa Canyon Bridge," *Earthquake Engineering & Structural Dynamics*, vol. 28, no. 7-8, pp. 879–897, 1999.

[15] B. Peeters, J. Maeck, and G. D. Roeck, "Vibration-based damage detection in civil engineering: excitation sources and temperature effects," *Smart Materials and Structures*, vol. 10, no. 3, pp. 518–527, 2001.

[16] A. Yan, G. Kerschen, P. D. Boe, and J. Golinval, "Structural damage diagnosis under varying environmental conditions—part I: a linear analysis," *Mechanical Systems and Signal Processing*, vol. 19, no. 4, pp. 847–864, 2005.

[17] J. Kullaa, "Elimination of environmental influences from damage-sensitive features in a structural health monitoring system," in *Structural Health Monitoring—The Demands and Challenges*, pp. 742–749, CRC Press, Palo Alto, Calif, USA, 2001.

[18] A. M. Yan, G. Kerschen, P. D. Boe, and J.-C. Golinval, "Structural damage diagnosis under varying environmental conditions—part II: local PCA for non-linear cases," *Mechanical Systems and Signal Processing*, vol. 19, no. 4, pp. 865–880, 2005.

[19] V. Meruane and W. Heylen, "Structural damage assessment under varying temperature conditions," *Structural Health Monitoring*, vol. 11, no. 3, pp. 345–357, 2012.

[20] R. Singh, A. Kainthola, and T. N. Singh, "Estimation of elastic constant of rocks using an ANFIS approach," *Applied Soft Computing*, vol. 12, no. 1, pp. 40–45, 2012.

[21] Z. Zhang and A. E. Aktan, "Application of modal flexibility and its derivatives in structural identification," *Research in Nondestructive Evaluation*, vol. 10, no. 1, pp. 43–61, 1998.

[22] T. Pham, *The influence of thermal effects on structural health monitoring of Attridge Drive Overpass [M.S. thesis]*, Department of Civil Engineering, University of Saskatchewan, Saskatchewan, Canada, 2009.

[23] S. N. Shoukry, G. W. William, B. Downie, and M. Y. Riad, "Effect of moisture and temperature on the mechanical properties of concrete," *Construction and Building Materials*, vol. 25, no. 2, pp. 688–696, 2011.

[24] R. W. Clough and J. Penzien, *Dynamics of Structure*, McGraw-Hill, New York, NY, USA, 2nd edition, 1993.

[25] Y. Xia, H. Hao, G. Zanardo, and A. Deeks, "Long term vibration monitoring of an RC slab: temperature and humidity effect," *Engineering Structures*, vol. 28, no. 3, pp. 441–452, 2006.

[26] R. D. Adams, P. Cawley, C. J. Pye, and B. J. Stone, "A vibration technique for nondestructively assessing the integrity of structures," *Journal of Mechanical Engineering Science*, vol. 20, no. 2, pp. 93–100, 1978.

[27] R. D. Blevins, *Formulas for Natural Frequency and Mode Shape*, Van Nostrand Reinhold, New York, NY, USA, 1979.

[28] C. Lanczos, *The Variational Principles of Mechanics*, Dover, New York, NY, USA, 4th edition, 1986.